Experimental overview on vorticity and polarization in heavy-ion collisions

Ilya Selyuzhenkov

(GSI, Darmstadt)

Terzo Incontro di Fisica con Ioni Pesanti alle Alte Energie 2021

Terzo incontro di fisica con ioni pesanti alle alte energie

25 November, 2021

Introduction

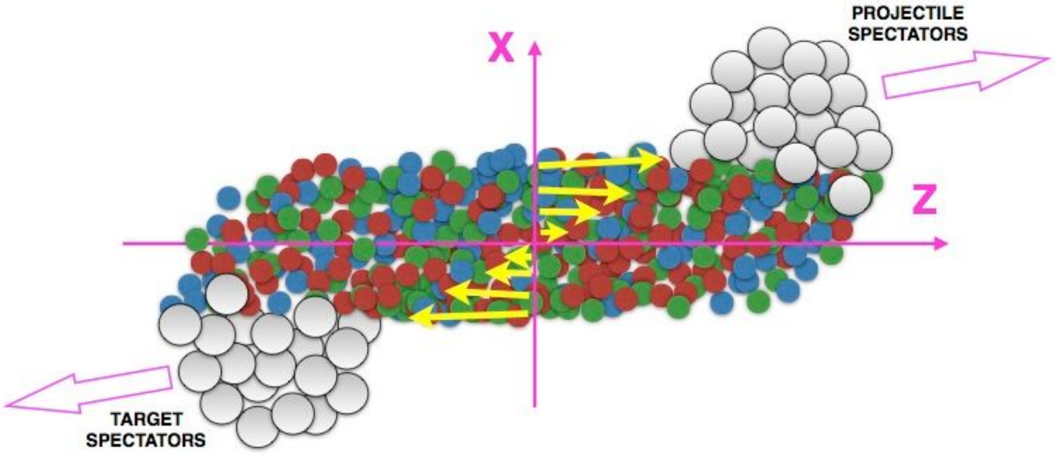

This overview is focused only on polarization effects induced by (fluid) velocity gradients resulting from:

- global orbital angular momentum
- collision geometry / collective expansion / anisotropic flow
- strong magnetic field induced by colliding charged nuclei

Non-central relativistic heavy ion collision (HIC)

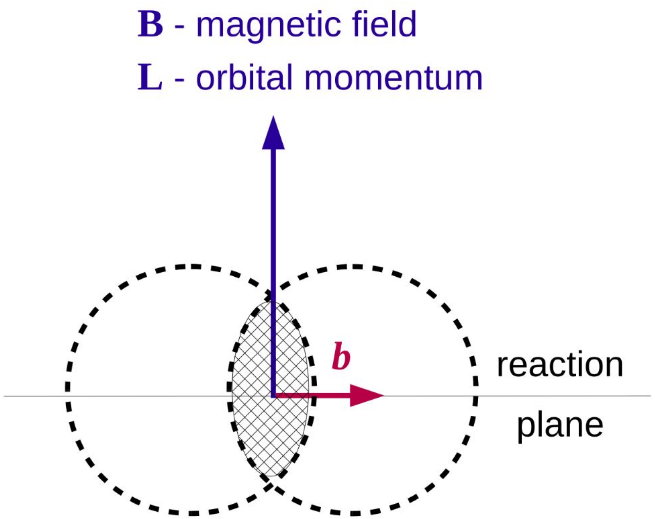

b – impact parameter

Colliding nuclei are moving out-of-list

- Overlapped area:
  non-uniform particle density
  and pressure gradient

- Large orbital angular momentum:

  $$L \sim bA\sqrt{s_{NN}} \sim 10^{4-6}\hbar$$

  Liang, Wang, PRL94:102301 (2005)
  Liang, JPG34:323 (2007)

- Strong magnetic field:

  $$\mathbf{B} \sim 10^{15}\,\mathrm{T} \qquad (e\mathbf{B} \sim 10^{4}\,\mathrm{MeV}^2)$$

  $$(\mu_{\mathrm{N}}\mathbf{B} \sim 100\,\mathrm{MeV})$$

  Rafelski, Müller PRL36:517 (1976)
  Kharzeev, PLB633:260 (2006)
  Kharzeev, McLerran, Warringa NPA803:227 (2008)

Global polarization: observables

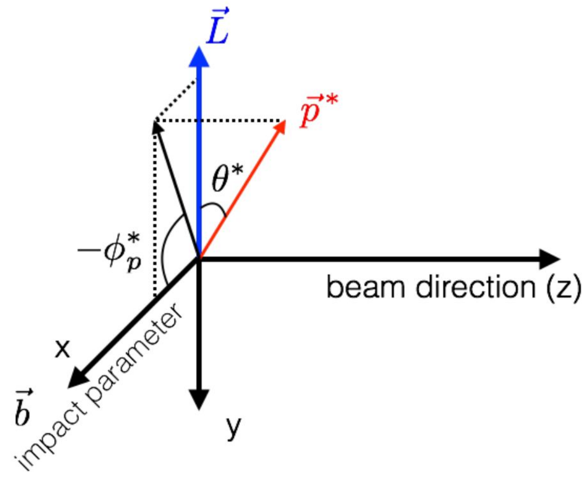

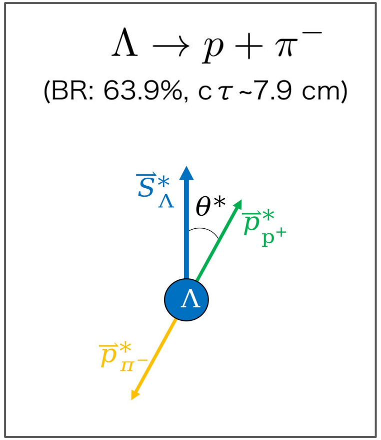

Orbital momentum is perpendicular to the reaction plane (opposite direction to y-axis - defines the polarization sign)

Angular distribution in the particle's decay rest frame:

$$\frac{dN}{d\cos\theta^*} \sim 1 + \alpha_H P_H \cos\theta^*$$

Estimate particle's spin direction from self analysing weak decay

For Λ: $\alpha_H = 0.732 / -0.758$ (updated PDG value in 2020)

Global polarization observable

$$P_H = \frac{8}{\pi \alpha_H} \langle \sin(\Psi_{RP} - \phi_p^*) \rangle$$

- Observable reflects P_y projection of the polarization
- Lorentz transformation of the orbital momentum to the rest frame of weak decay is not taken into account
  [W. Florkowski, R. Ryblewski, 2102.02890 [hep-ph]]

Global polarization: measurement techniques

$$\Lambda \to p + \pi^-$$

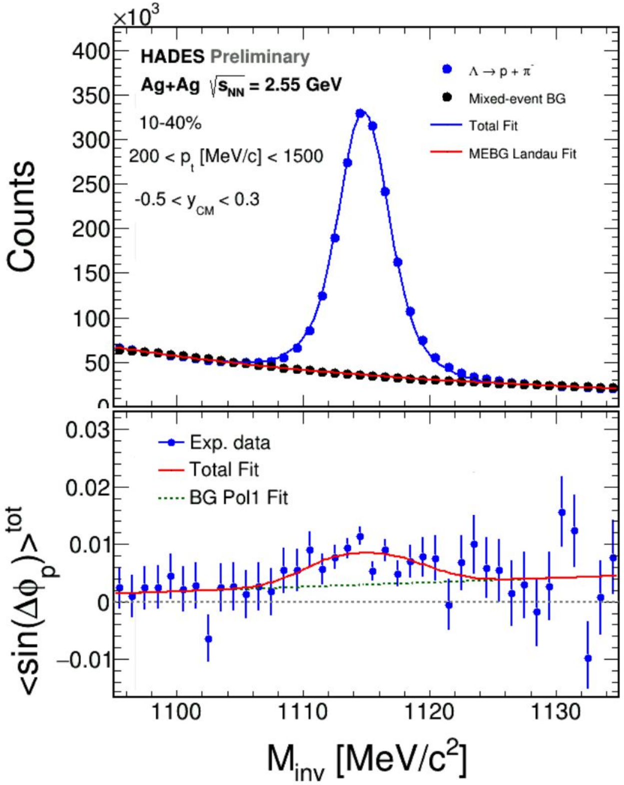

$$P_H = \frac{8}{\pi \alpha_H} \langle \sin(\Psi_{RP} - \phi_p^*) \rangle$$

Reaction plane is not known → use spector deflection direction

Strong elliptic flow cannot be used:
need to know direction of the orbital momentum (1st harmonic plane)

$$P_{\mathrm{H}} = \frac{8}{\pi \alpha_{\mathrm{H}}} \frac{\langle \sin(\Psi_1 - \phi_p^*) \rangle}{\mathrm{Res}(\Psi_1)}$$

Experimental difficulties:
combinatorial background in a few body decay reconstruction
can dilute the signal (if unpolarized)
or can result in additionally correlation
(e.g. due to directed flow coupled to one of the decay products)

Global polarization: reaction plane orientation & resolution

$$P_{\mathrm{H}} = \frac{8}{\pi \alpha_{\mathrm{H}}} \frac{\langle \sin(\Psi_1 - \phi_p^*) \rangle}{\mathrm{Res}(\Psi_1)}$$

HADES @GSI

HADES, PRL 125 (2020) 262301

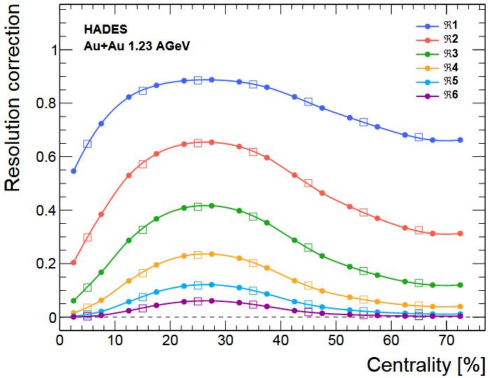

STAR @ RHIC

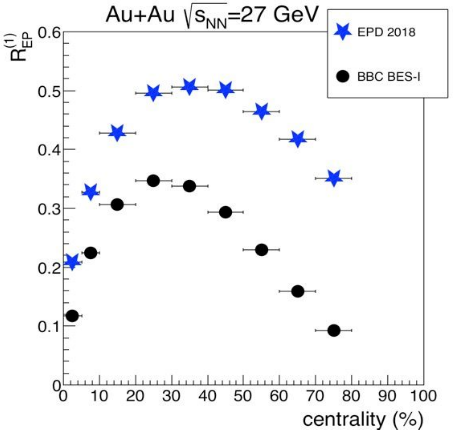

ALICE @ LHC

ALICE PRC 101 (2020) 4, 044611

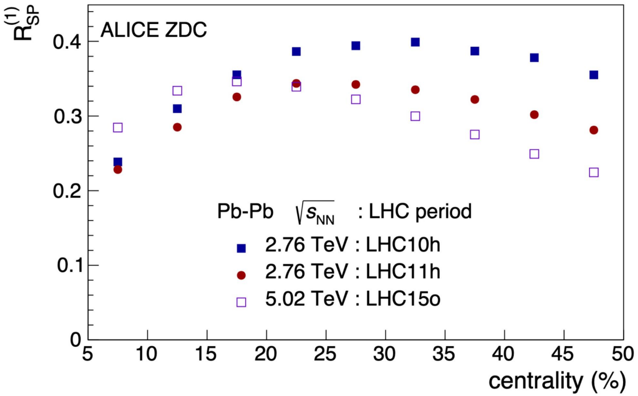

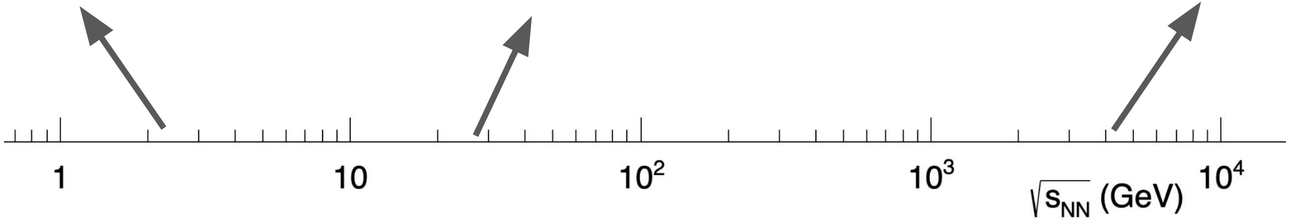

First preliminary results by STAR at Quark Matter 2005

STAR [I. Selyuzhenkov], Quark Matter 2005

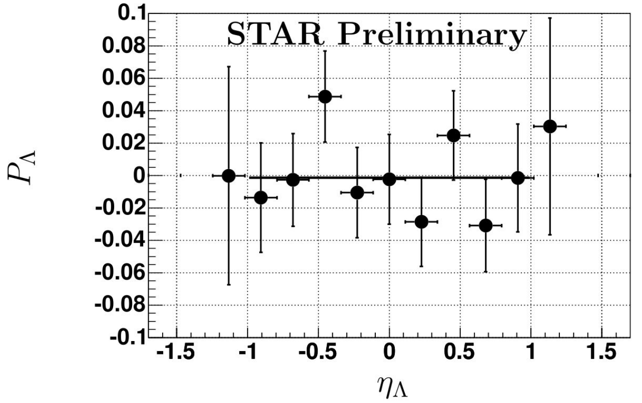

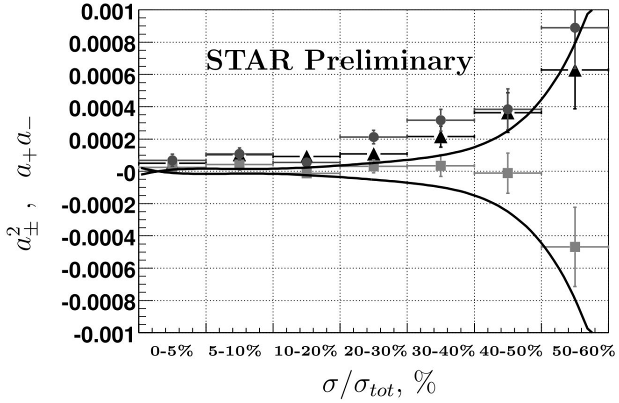

Global polarization and parity violation study in Au+Au collisions

Ilya Selyuzhenkov for the STAR Collaboration

Department of Physics and Astronomy, Wayne State University, USA

QM2005 proceedings: [Rom.Rep.Phys. 58 (2006) 049-054]

4 Summary

The full statistics for the STAR Au+Au data at $\sqrt{s_{NN}} = 62$ GeV for strange hyperons have been analyzed. The obtained upper limit for the global polarization of Λ hyperon, $P_\Lambda = (-1.44 \pm 9.66) \times 10^{-3}$, is far below the value predicted in [2].

Although the systematic uncertainties have not been yet clearly understood, the current analysis is capable of setting an upper limit on the effect of strong C and CP violation in nucleus-nucleus collisions discussed in [1].

[1] D. Kharzeev hep-ph/0406125 (2004)

[2] Z.-T. Liang, X.-N. Wang Phys. Rev. Lett. **94**, 102301 (2005),
S.A. Voloshin nucl-th/0410089 (2004),
Z.-T. Liang, X.-N. Wang nucl-th/0411101 (2004)

Global polarization: overview of world data

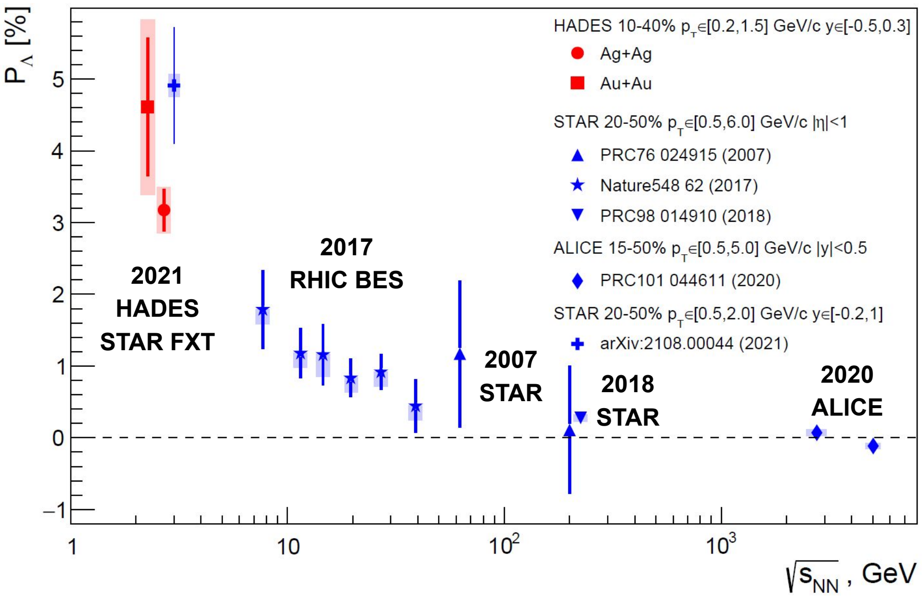

Particle / anti-particle yield

Figure by A. Andronic

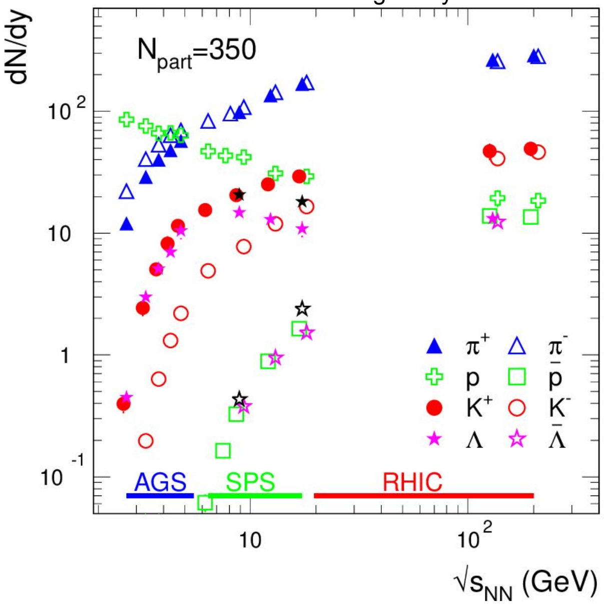

- > 15 years of experimental effort by STAR, ALICE, and HADES Collaborations
- Covers collision energy range from 2.4 GeV up to 5.02 TeV

Global polarization: collision energy dependence

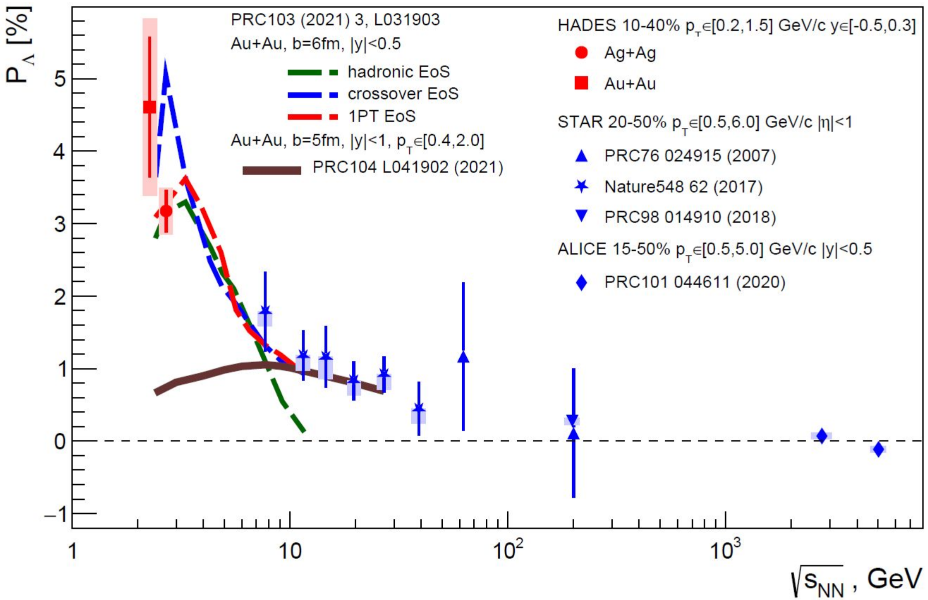

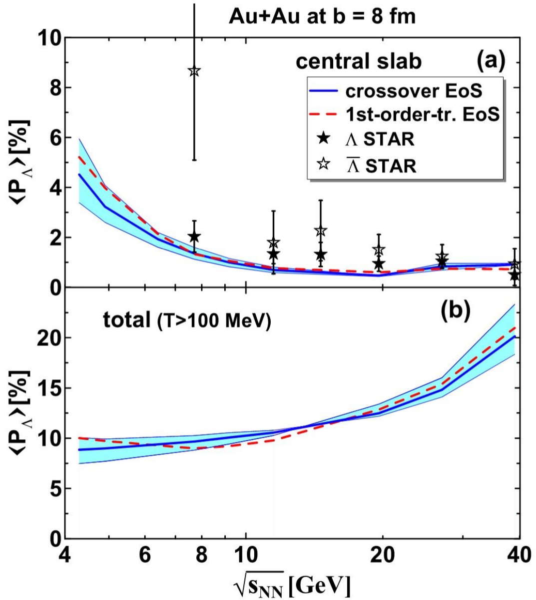

- Decreasing with collision energy if measured at midrapidity
- Maximum polarization at ~ 3 GeV, model predictions diverge
- LHC region to be explored with high statistics from Run3

Global polarization: centrality dependence

HADES @GSI

Model: O. Vitiuk et.al. Phys.Lett.B 803 (2020) 135298

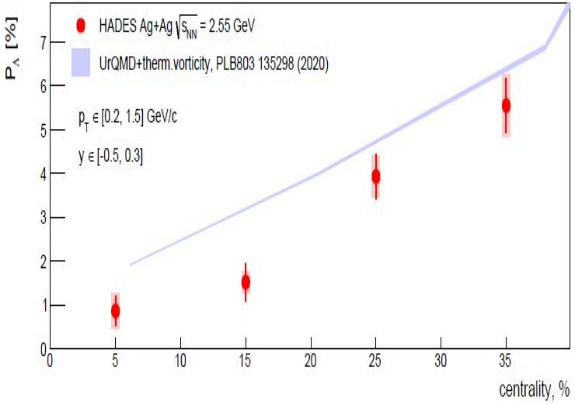

STAR @ RHIC

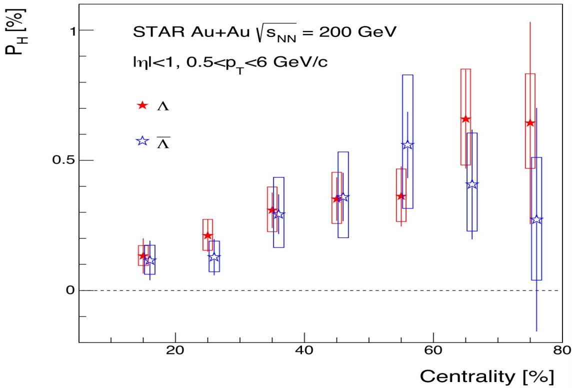

theory

Y. Jiang et.al. PRC 94 (2016) 4, 044910

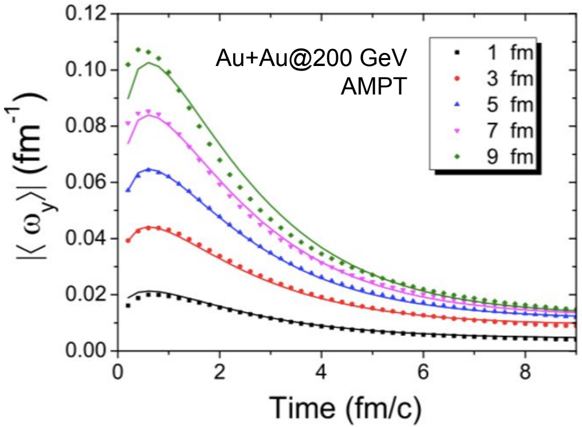

Strong centrality dependence reflecting the change of the orbital angular momentum / vorticity increase

Global polarization: rapidity dependence

HADES @GSI

Model: O. Vitiuk et.al. Phys.Lett.B 803 (2020) 135298

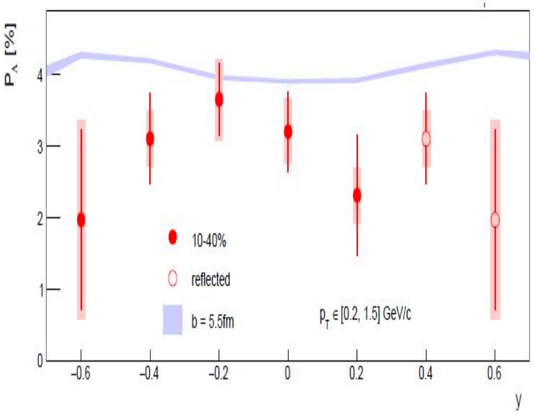

STAR @ RHIC

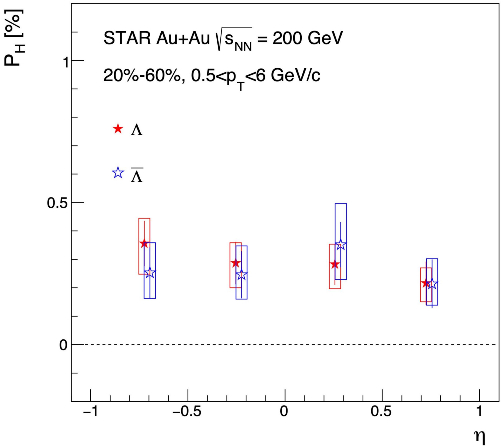

theory

Liang, et. al. Chin.Phys.C 45 (2021) 1, 014102

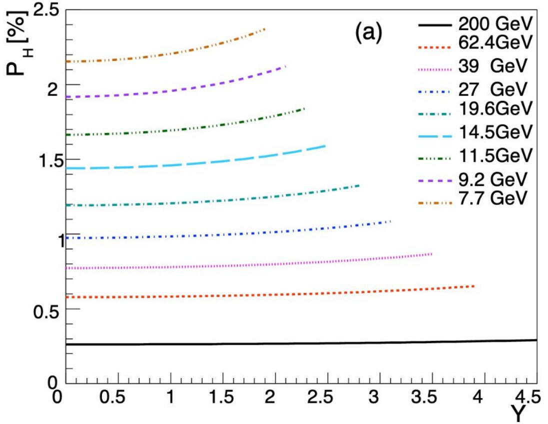

BUR2020, STAR Note SN0755

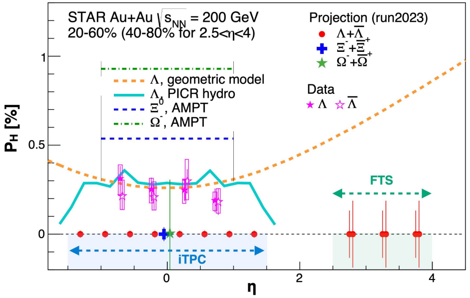

- No significant rapidity dependence at all energies
- At low energies (fixed target experiments) reach beam rapidity

Global polarization: p_T and centrality dependence

HADES @GSI

STAR @ RHIC

theory

Model: O. Vitiuk et.al. Phys.Lett.B 803 (2020) 135298

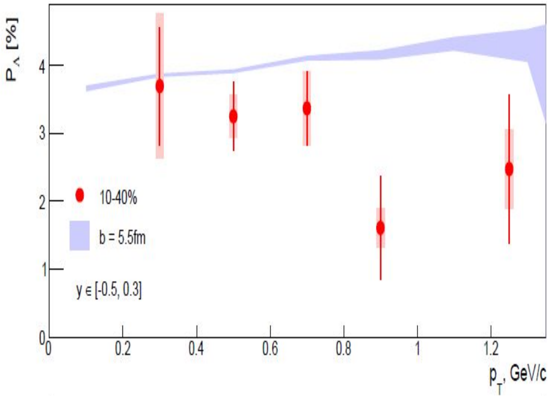

Hydro: F. Becattini, Karpenko PRL 120 (2018) 1, 012302

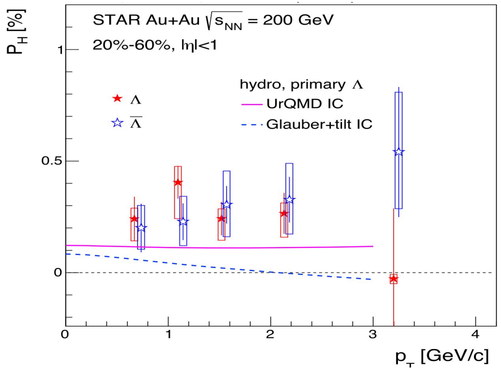

S. Ryu et.al. arXiv:2106.08125 [nucl-th]

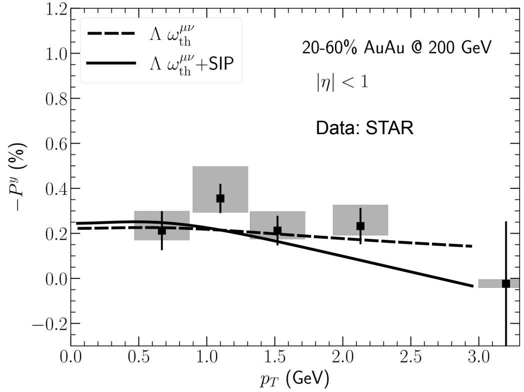

No significant p_T dependence at all energies

Measurements at high p_T can provide strong constraints (thermal shear contribution grows quadratically with p_T)

Global polarization: connection to the directed flow slope

Global polarization

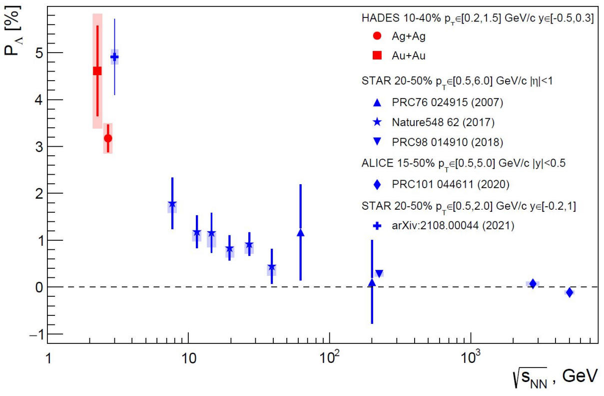

Slope of directed flow (dv_1/dy) at midrapidity

Low energy region (HADES, STAR FXT)

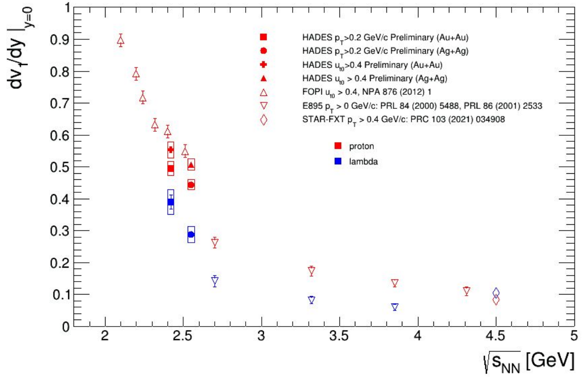

High energy region (RHIC / LHC)

Voloshin, EPJ Web Conf. 171 (2018) 07002

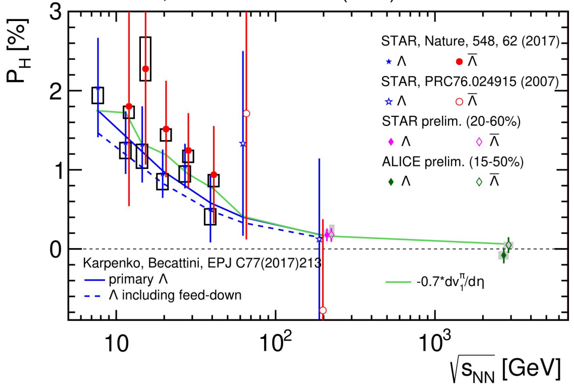

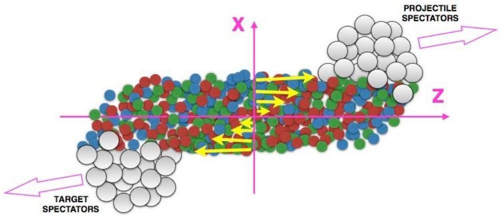

Connection between source of directed flow (velocity profile, initial tilt, dipole flow, viscosity) and of polarization (orbital momentum / vorticity)

F. Becattini et.al., Eur.Phys.J.C 75 (2015) 9

Global polarization: hyperon - anti-hyperon difference

F. Becattini and M. A. Lisa, Ann. Rev. Nucl. Part. Sci.70, 395 (2020)

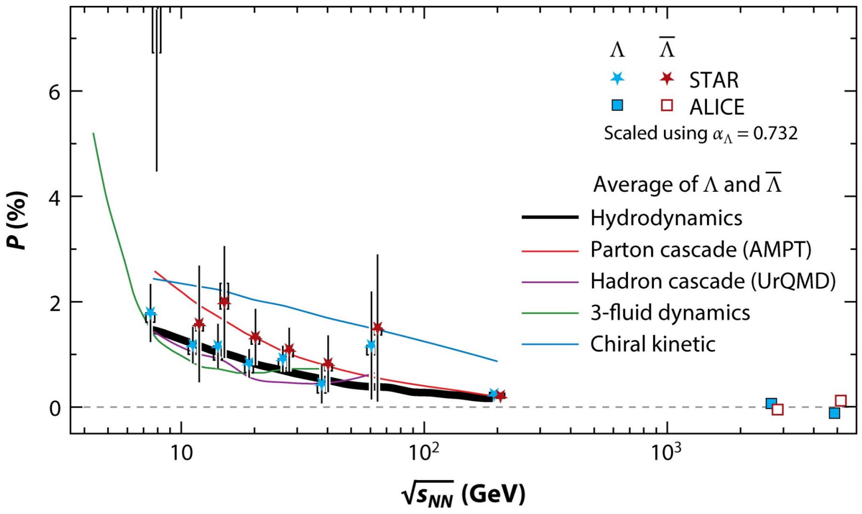

Difference between lambda and anti-lambda is sensitive to

- magnetic field
- Baryon chemical potential

$$P_{\Lambda(\bar{\Lambda})} \simeq \frac{1}{2}\frac{\omega}{T} \pm \frac{\mu_\Lambda B}{T}$$

Global polarization: probing the strong magnetic field?

Magnetic field evolution

L. McLerran and V. Skokov, NPA 929, 184 (2014)

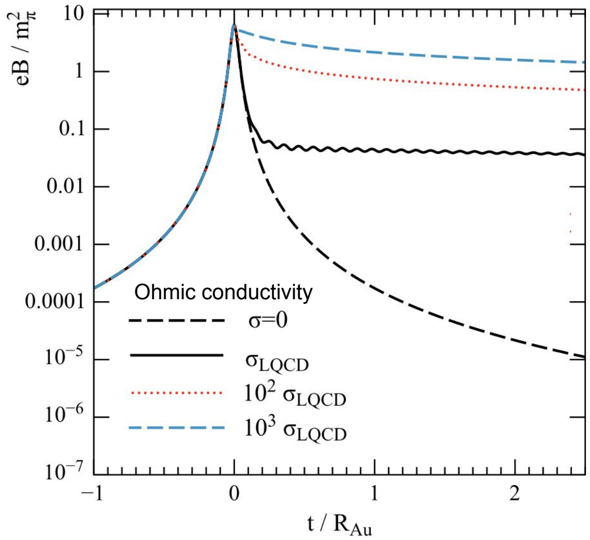

Separating contribution from vorticity and magnetic field

$$P_{\Lambda(\bar{\Lambda})} \simeq \frac{1}{2}\frac{\omega}{T} \pm \frac{\mu_\Lambda B}{T}$$

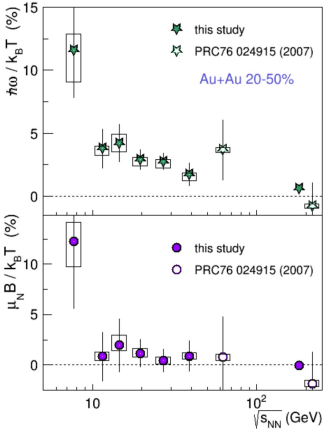

Estimates of magnetic field from global polarization

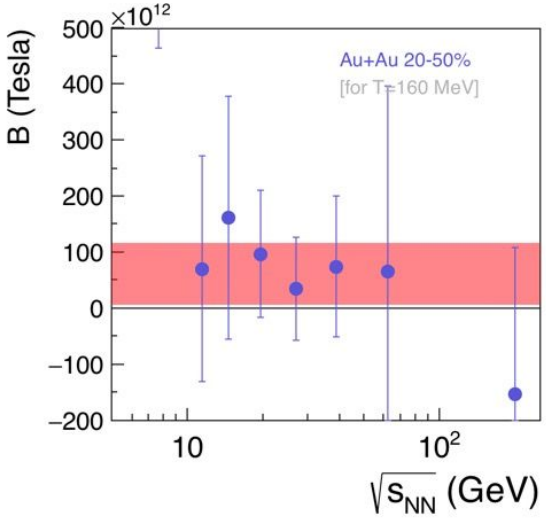

$B = 6.0 \pm 5.5 \times 10^{13}$ T $\approx 0.6 \pm 0.5\ m_\pi^2$

No significant effect from the magnetic field.
Velocity gradients (vorticity ,..) dominates the measured polarization

Global polarization: connection to chiral effects

Chiral separation effect (CSE)

Separation of axial charge along the magnetic field

Axial current: $\mathbf{J}_5 \propto e\mu_v \mathbf{B}$

μ_v vector chemical potential

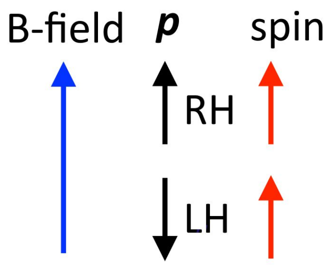

$e\mu_v > 0$ ($e\mu_v < 0$):

spins of particles (antiparticles) aligned with $\mathbf{B}$ direction

$$\mu_v/T \propto \frac{\langle N_+ - N_- \rangle}{\langle N_+ + N_- \rangle}$$

STAR, PRC98, 014910 (2018)

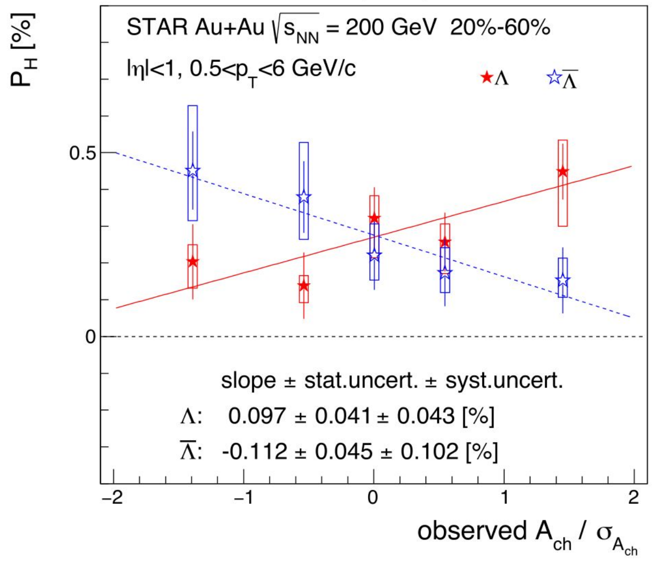

Not enough statistics yet: (1–2σ) precision

D.E. Kharzeev et.al. Prog.Part.Nucl.Phys. 88 (2016) 1-28

Multi-strange hyperons: Ξ, Ω and feed-down to Λ polarization

I. Karpenko and F. Becattini, EPJ. C 77 (2017) 213

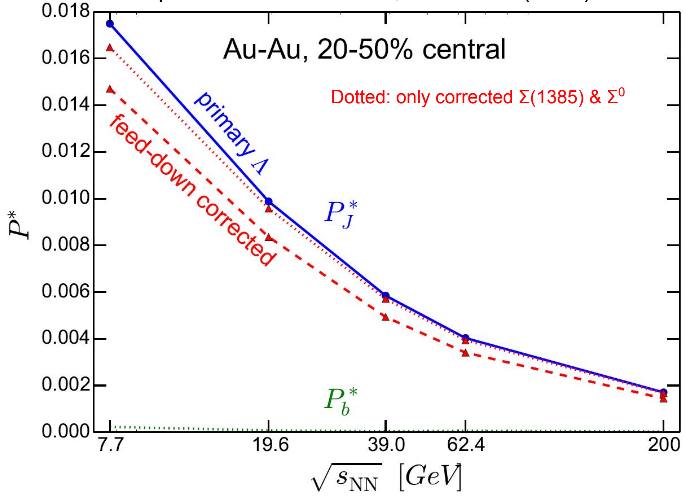

STAR, PRL126, 162301 (2021)

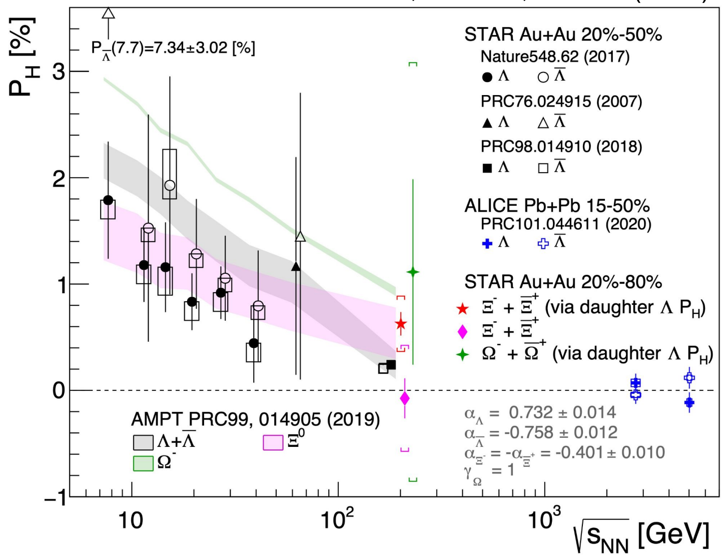

T.D. Lee and C.N. Yang, Phys. Rev.108.1645 (1957)

$$\mathbf{P}_\Lambda^* = \frac{(\alpha_\Xi + \mathbf{P}_\Xi^* \cdot \hat{\boldsymbol{p}}_\Lambda^*)\hat{\boldsymbol{p}}_\Lambda^* + \beta_\Xi \mathbf{P}_\Xi^* \times \hat{\boldsymbol{p}}_\Lambda^* + \gamma_\Xi \hat{\boldsymbol{p}}_\Lambda^* \times (\mathbf{P}_\Xi^* \times \hat{\boldsymbol{p}}_\Lambda^*)}{1 + \alpha_\Xi \mathbf{P}_\Xi^* \cdot \hat{\boldsymbol{p}}_\Lambda^*}$$

$$\alpha^2 + \beta^2 + \gamma^2 = 1$$

$$\mathbf{P}_\Lambda^* = C_{\Xi^-\Lambda} \mathbf{P}_\Xi^* = \tfrac{1}{3}\left(1 + 2\gamma_\Xi\right) \mathbf{P}_\Xi^*. \qquad C_{\Xi^-\Lambda} = +0.944$$

$$\mathbf{P}_\Lambda^* = C_{\Omega^-\Lambda} \mathbf{P}_\Omega^* = \tfrac{1}{5}\left(1 + 4\gamma_\Omega\right) \mathbf{P}_\Omega^*$$

Thermal model: $P_\Lambda = P_\Xi = 3/5 * P_\Omega$

hyperon	decay mode	α_H	magnetic moment μ_H	spin
Λ (uds)	$\Lambda \to p\pi^-$ (BR: 63.9%)	0.732	-0.613	1/2
Ξ^- (dss)	$\Xi^- \to \Lambda\pi^-$ (BR: 99.9%)	-0.401	-0.6507	1/2
Ω^- (sss)	$\Omega^- \to \Lambda K^-$ (BR: 67.8%)	0.0157	-2.02	3/2

Longitudinal polarization: observable

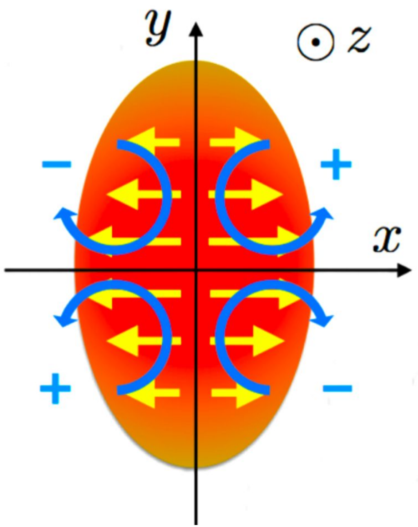

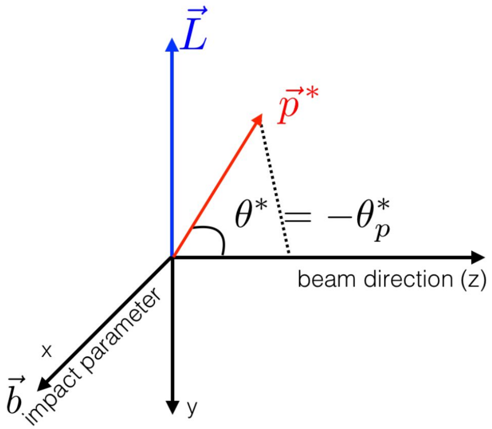

In-plane elliptic flow generates local vorticities along beam axis

Observable for a perfect detector

$$P_z = \frac{3\langle\cos\theta_p^*\rangle}{\alpha_{\mathrm{H}}}$$

Experimental observable
(case of limited acceptance)

$$P_z = \frac{\langle\cos\theta_p^*\rangle}{\alpha_{\mathrm{H}}\langle(\cos\theta_p^*)^2\rangle}$$

Projection on the elliptic flow plane

$$P_{z,s2} = < P_z \sin(2\varphi - 2\Psi_2) >$$

Longitudinal polarization: vorticity vs. thermal shear

STAR @ RHIC

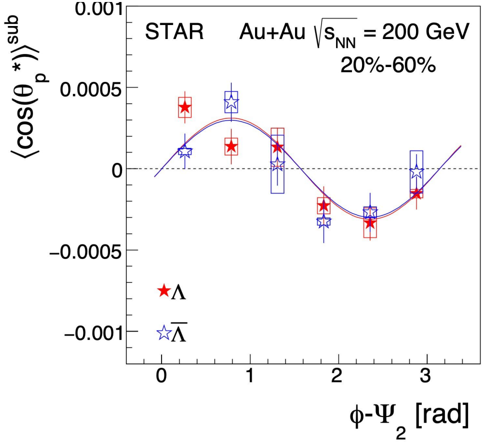

ALICE @ LHC

arXiv:2107.11183

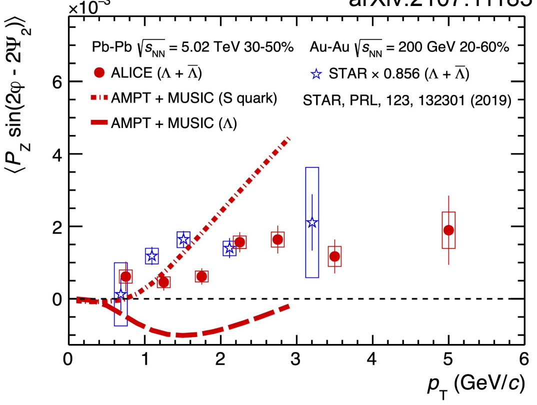

hydrodynamic predictions
F. Becattini et.al arXiv:2103.14621

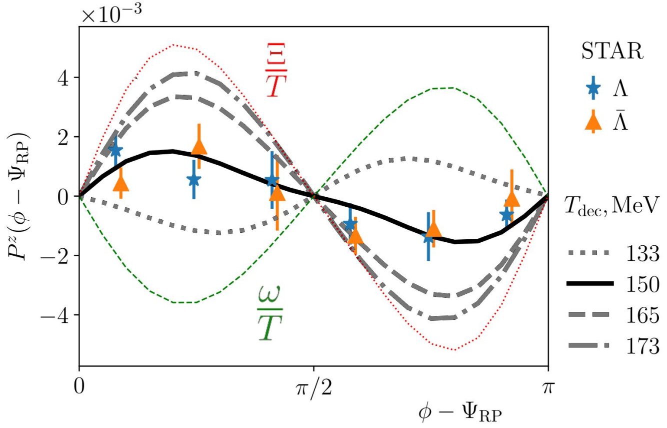

ALICE & STAR observes similar pattern & magnitude

Same approach also applicable for global polarization

thermal vorticity $\varpi_{\mu\nu} = -\frac{1}{2}\left(\partial_\mu\beta_\nu - \partial_\nu\beta_\mu\right)$

thermal shear tensor $\xi_{\mu\nu} = \frac{1}{2}\left(\partial_\mu\beta_\nu + \partial_\nu\beta_\mu\right)$

at very high energy
isothermal local equilibrium

$\beta^\mu = u^\mu/T$

$\omega_{\rho\sigma} = \frac{1}{2}\left(\partial_\sigma u_\rho - \partial_\rho u_\sigma\right)$

$\Xi_{\rho\sigma} = \frac{1}{2}\left(\partial_\sigma u_\rho + \partial_\rho u_\sigma\right)$

Confirms local thermodynamic equilibrium / QGP as a quasi-ideal fluid

New polarization observables: ring structure

Symmetric nuclei collisions:
Longitudinal gradient of transverse flow (and temperature)
→ ring structure of vorticity

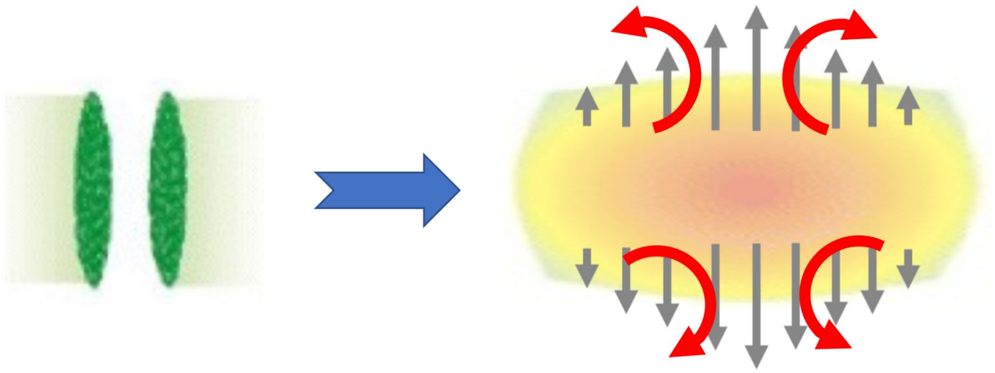

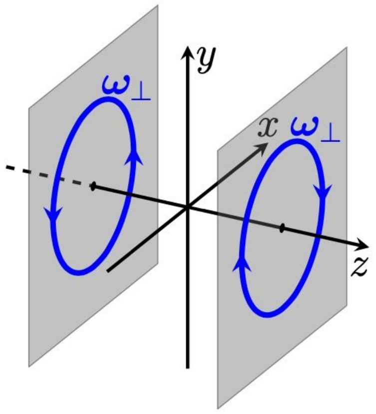

Xia, Li, Tang, Wang PRC 98, 024905 (2018)

- Helicity separation in heavy-ion collisions (QGSM)
  Baznat, Gudima, Sorin, Teryaev PRC88, 061901(R) (2013)
- Vorticity and hydrodynamic helicity in heavy-ion collisions in the HSD model
  Teraev & Usubov PRC92 014906 (2015)
- Femto-vortex sheets and hyperon polarization in heavy-ion collisions (QGSM)
  Baznat, Gudima, Sorin, Teryaev PRC93, 031902(R) (2016)
- Vorticity in heavy-ion collisions at the JINR NICA (3FD)
  Ivanov & Soldatov, PRC 95, 054915 (2017)
- Vortex rings in fragmentation regions in heavy-ion collisions at √sNN = 39 GeV (3FD)
  Ivanov & Soldatov PRC97, 044915 (2018)
- Vorticity structure and polarization of Λ hyperons in heavy-ion collisions (PHSD)
  Zinchenko, Sorin, Teryaev, Baznat DSPIN-2019 (2020)

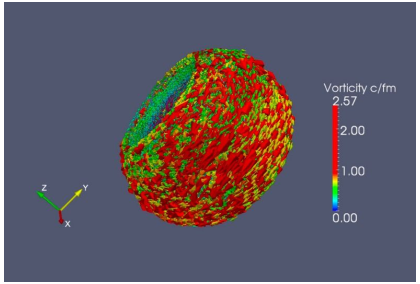

Baznat, Gudima, Sorin, Teryaev
PRC93, 031902(R) (2016)

New observables: ring structure (asymmetric systems)

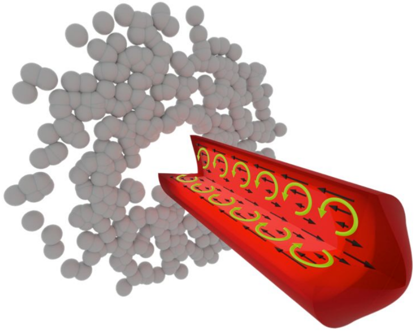

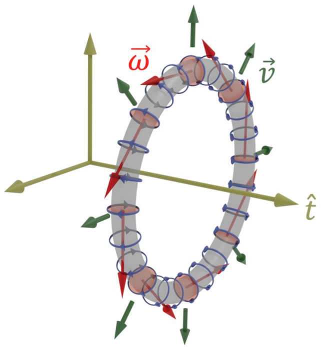

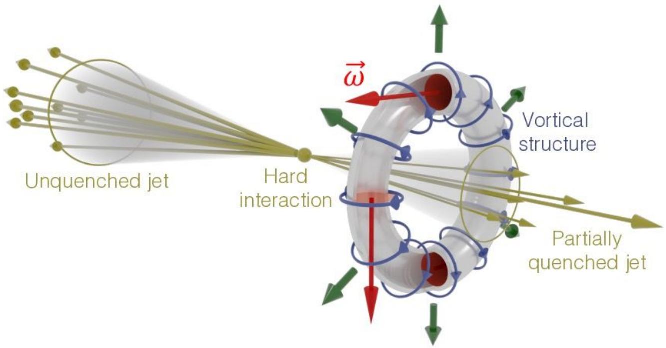

vortex rings, when proton penetrates through a nucleus

S. Voloshin, EPJ Web Conf.171, 07002 (2018)
M. Lisa et. al., PRC 104, (2021) L011901

Vortex rings around quenched jet direction excites vortical flow pattern along its trajectory

B. Betz et.al., PRC76 (2007) 044901
Y. Tachibana and T. Hirano, NPA904 (2013) 1023
W. Serenone, et.al. PLB 820 (2021) 136500

Study fluid structure at the extremes of rapidity

Summary

Polarization probes the hydrodynamically expanding system at finest level of detail:

- More than 15 years of experimental activities and many new recent measurements:
  - Observe non-zero global and local polarizations, other observables proposed
  - Results cover 3 orders of magnitude in collision energy for different hyperons (Λ,Ξ, Ω)
  - Particle - anti-particle splitting (effect of magnetic field) have not yet been observed

- At high energies (RHIC & LHC)
  - precision multi-differential measurements at top RHIC and LHC energy
  - Similar local polarization at RHIC and LHC, global polarization too small at the LHC → RUN3
  - “Sign problem” can be explained by non-vortical thermal shear
  - Understanding data for the global spin alignment of ϕ-meson and K^{*0} (see backup)

- (New) low energies (HADES and STAR FXT)
  - Data show maximum polarization ~ 2.5 - 3 GeV
    quantitatively predicted by 3-fluid hydro, but model predictions diverge
  - No rapidity dependence over entire rapidity range

Outlook

Several other directions to explore

- Longitudinal polarization for higher-order harmonics
- Understand better connection with the directed flow slope at midrapidy
- Toroidal vorticity structures expected in head-on and asymmetric collisions at all energies
  - STAR/collider – possible with forward upgrade; also possible at the LHCb
  - vortex toroids produced by “disturbances”
  - proton through nuclei & jets through QGP
  - Spin-spin correlations to probe scale of vortical texture of the QGP
- Vorticity and charm quarks: global spin alignment of J/Ψ

Ongoing / planned experimental programs

LHC Run-3 (ALICE, CMS, ATLAS, LHCb)
STAR BES-II + Run 2023-2025
HADES
NA61/SHINE
Future experiments: FAIR, NICA, et. al.

BACKUP

Spin alignment of vector mesons

$$\frac{dN_1}{d\cos\theta^*} = \frac{3}{4}\left[1 + \rho_{00} + (3\rho_{00} - 1)\ \cos^2\theta^*\right]$$

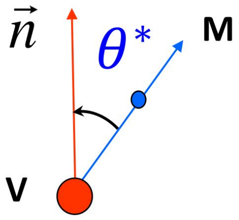

Spin alignment:

$$\rho_{00} \neq \frac{1}{3}$$

Naïve estimation:

$$\rho_{00} - \frac{1}{3} \sim P_H^2 \sim 10^{-4}$$

Experimental result:

$$\rho_{00} - \frac{1}{3} \sim 10^{-1}$$

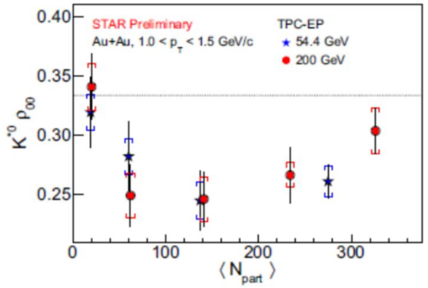

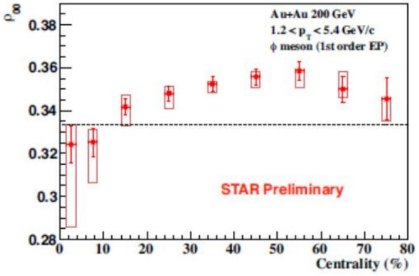

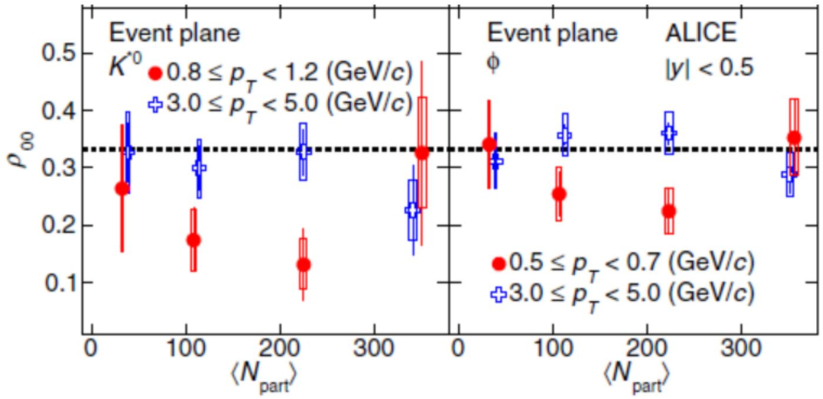

X.L. Sheng

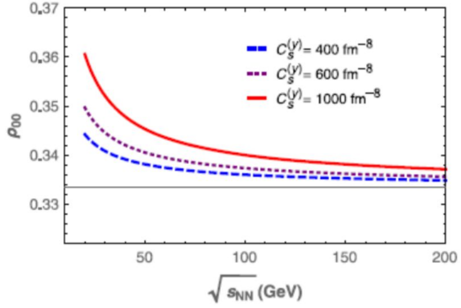

Global spin alignment at the LHC and RHIC

ALICE, PRL125, 012301 (2020)

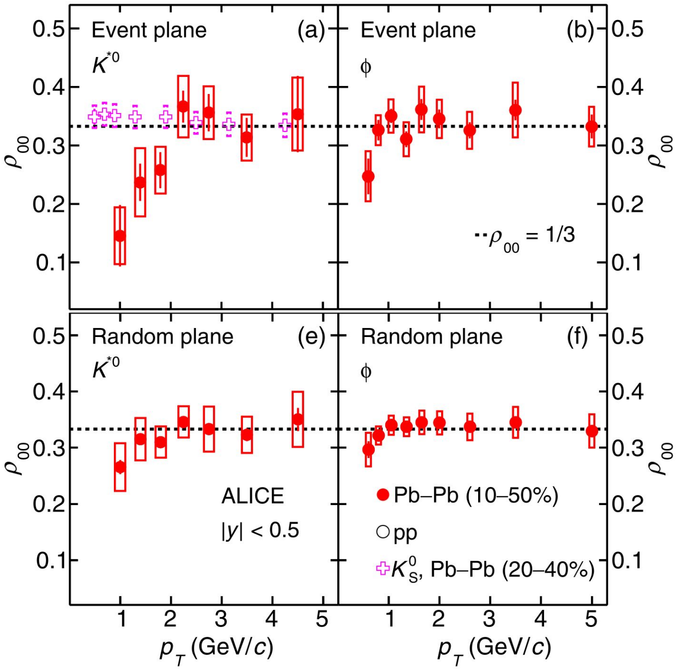

S. Singha (STAR), QM2019

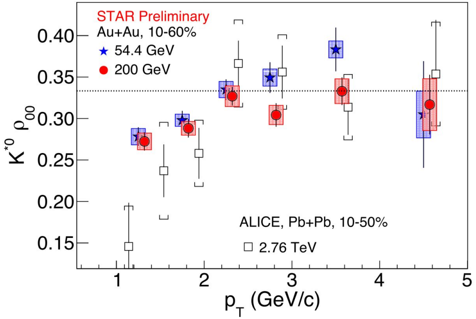

C. Zhou (STAR), QM2018

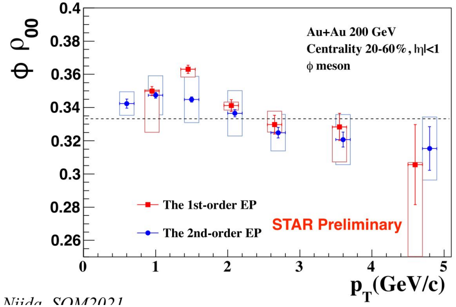

ρ_{00} >1/3 for φ below 1/3 for low p_T → different from the LHC

Large deviation from 1/3 cannot be explained by vorticity

Over polarization observables: vortical spots

L. Pang, H. Petersen, Q. Wang, X-N Wang, PRL117 (2016) 192301

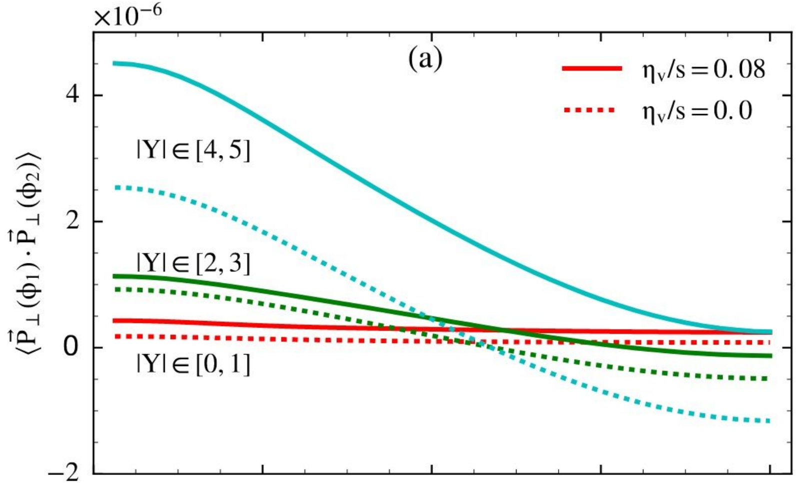

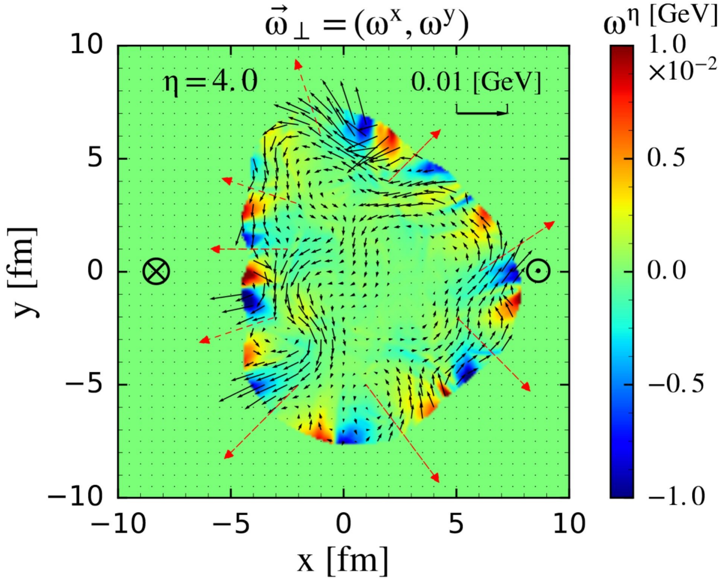

"vortical spots" fluctuating in strength/position/orientation event-to-event

STAR FXT: Global polarization & rapidity dependence

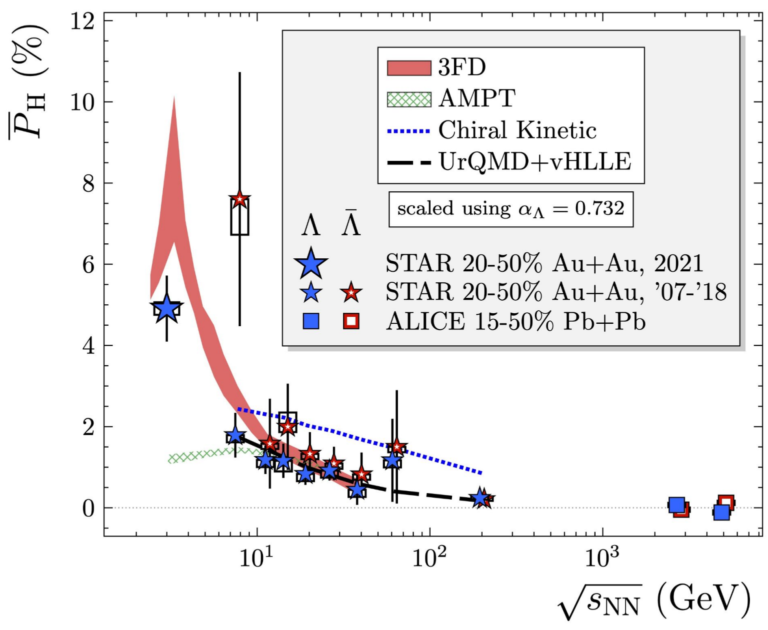

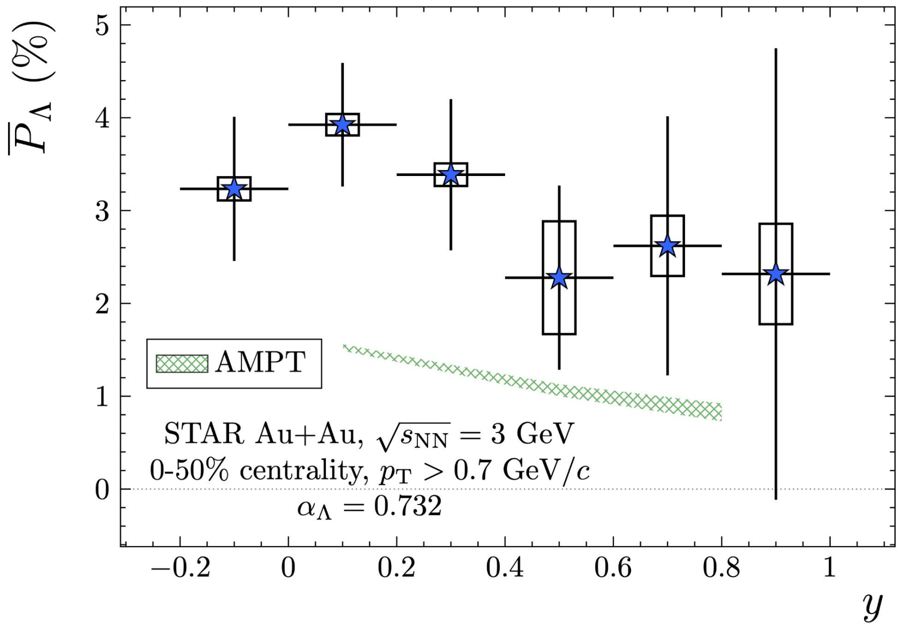

Local polarization and isothermal local equilibrium in relativistic heavy ion collisions

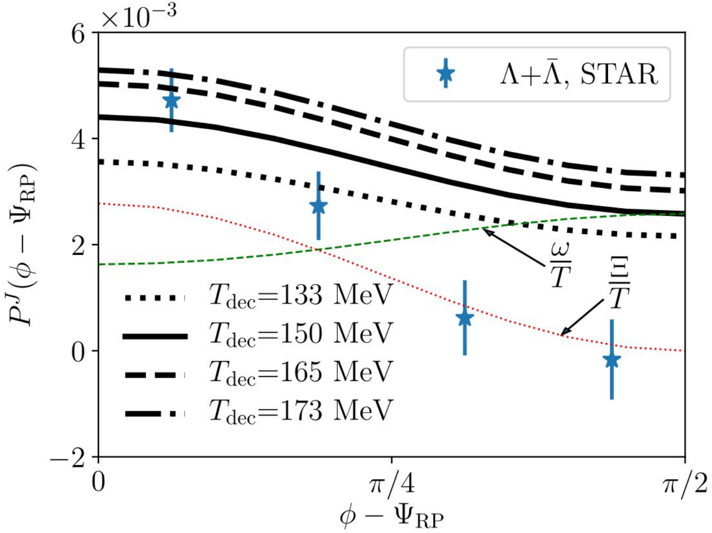

FIG. 5. Λ polarization component along the global angular momentum, as a function of the azimuthal angle ϕ, computed with vHLLE for 20-60% Au-Au collisions at $\sqrt{s_{\rm NN}}$ = 200 GeV. Experimental data points are taken from [41].

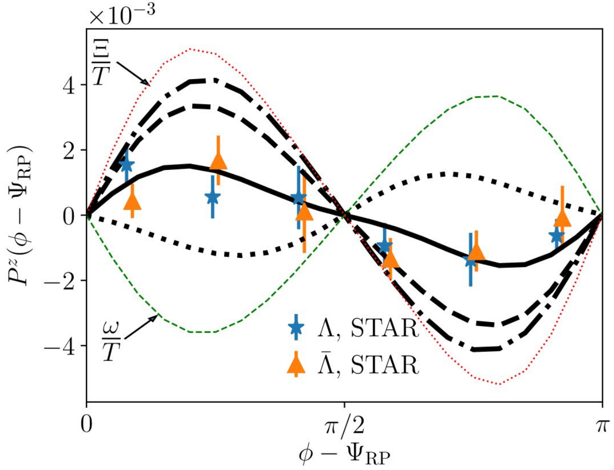

FIG. 6. Λ polarization component along the beam direction, as a function of the azimuthal angle ϕ, computed with vHLLE for 20-60% Au-Au collisions at $\sqrt{s_{\rm NN}}$ = 200 GeV. Experimental data points are taken from [37] and conversion from $\langle \cos\theta_p^* \rangle$ to P_H is performed using $\alpha_{\rm H} = 0.732$ [43]. Error bars represent the sum of statistical and systematic uncertainties. Line styles correspond to different decoupling temperatures as in Fig. 5.

F. Becattini et.al. arXiv:2103.14621 [nucl-th]

Rapidity dependence of the global polarization

Xie, Wang, Csernei RPJ(2020)80:39

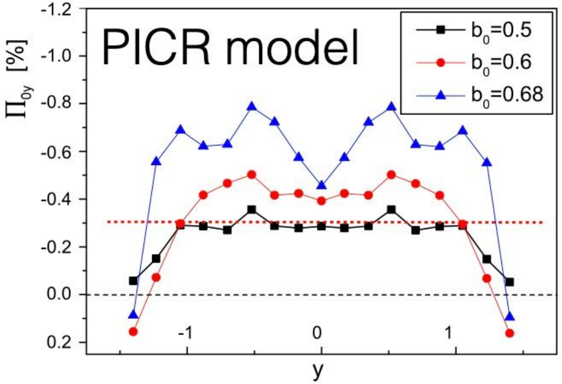

Wei,Deng,Huang PRC99(2019)014905

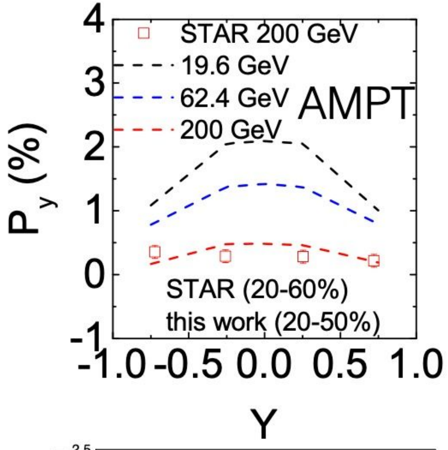

Feng, Huang PRC93(2016)064907

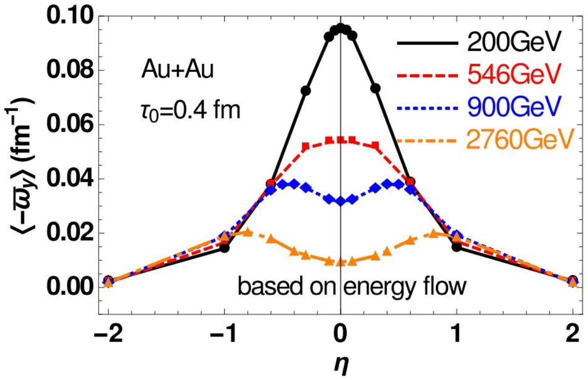

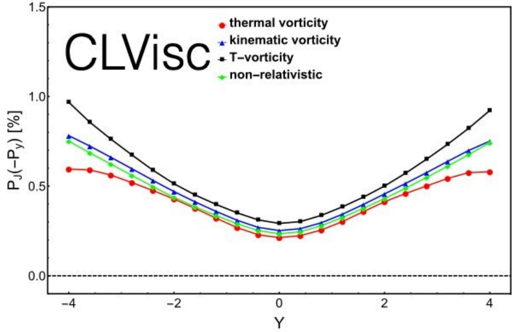

Wu et al, Phys. Rev. Res. 1 (2019) 033058

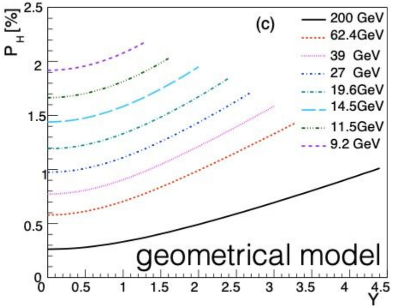

Liang, et al arXiv:1912.10223
Chin.Phys.C 45 (2021) 1, 014102

Most models reproduce midrapidity polarization, while predictions outside vary significantly

ALICE @ LHC projections for global polarization

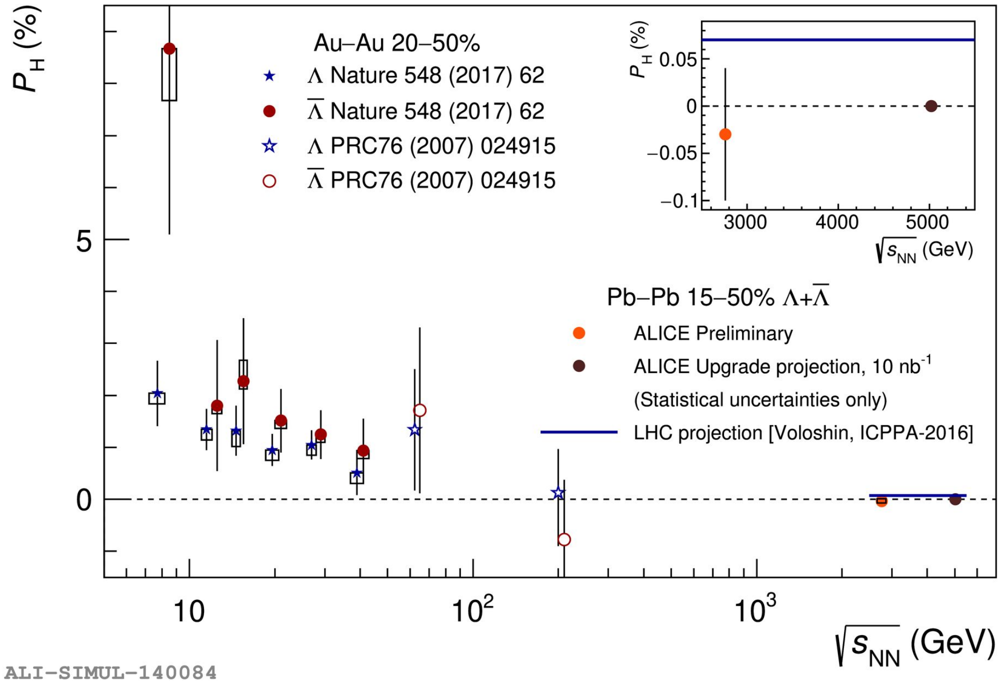

Directed flow and orbital angular momentum

F. Becattini et.al., Eur.Phys.J.C 75 (2015) 9

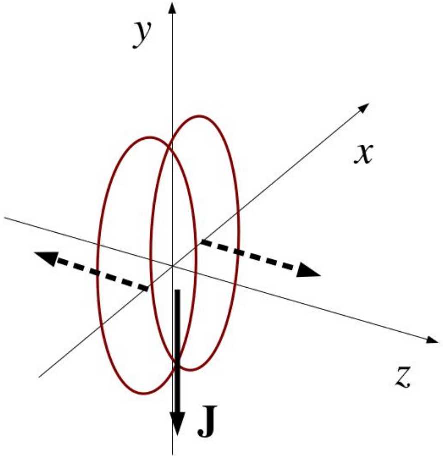

$$J^y = -\tau_0 \int \mathrm{d}x\,\mathrm{d}y\,\mathrm{d}\eta\; x\,\varepsilon(x,y,\eta)\,\sinh\eta$$

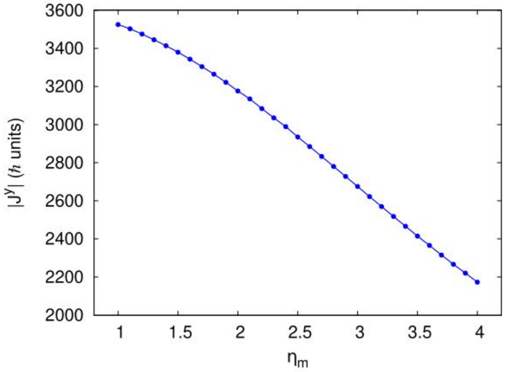

Figure 9: Angular momentum (in $\hbar$ units) of the plasma with Bjorken initial conditions as a function of the parameter η_m.

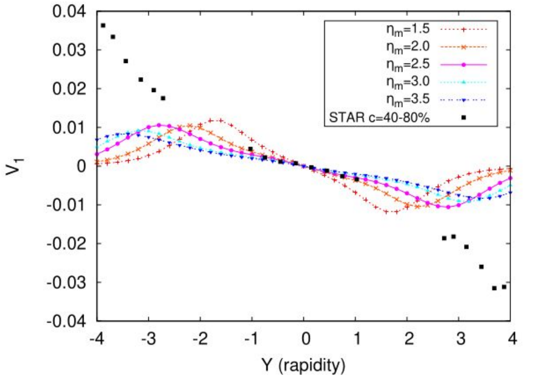

Figure 6: (color online) Directed flow of pions for different values of η_m parameter with $\eta/s = 0.1$ compared with STAR data [22].

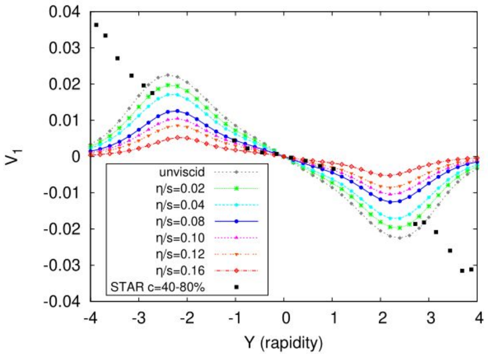

Figure 7: (color online) Directed flow of pions for different values of η/s with $\eta_m = 2.0$ compared with STAR data [22].

$$W_N(x,y,\eta) = 2\,\left(T_1(x,y)f_-(\eta) + T_2(x,y)f_+(\eta)\right)$$

$$\varepsilon(x,y,\eta) = \varepsilon_0\,W(x,y,\eta)\,H(\eta),$$

$$f_-(\eta) = \begin{cases} 1 & \eta < -\eta_m \\ \dfrac{-\eta+\eta_m}{2\eta_m} & -\eta_m \le \eta \le \eta_m \\ 0 & \eta > \eta_m \end{cases} \qquad f_+(\eta) = \begin{cases} 0 & \eta < -\eta_m \\ \dfrac{\eta+\eta_m}{2\eta_m} & -\eta_m \le \eta \le \eta_m \\ 1 & \eta > \eta_m \end{cases}$$